

Rate Studies on the Release of Terminal Alkynes from Indenylruthenium(II) Vinylidene Complexes. Implications on the Mechanism of η^1 -Vinylidene into η^2 -Alkyne Isomerization

Mauro Bassetti,^{*,†} Victorio Cadierno,^{*,‡} José Gimeno,[‡] and Chiara Pasquini[†]

Istituto CNR di Metodologie Chimiche and Dipartimento di Chimica, Università "La Sapienza", Piazzale A. Moro 5, I-00185 Roma, Italy, and Departamento de Química Orgánica e Inorgánica, Instituto de Química Organometálica "Enrique Moles" (Unidad Asociada al CSIC), Universidad de Oviedo, C/Julian Clavería 8, E-33071 Oviedo, Principado de Asturias, Spain

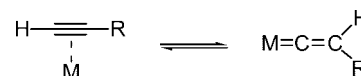
Received May 28, 2008

The indenylruthenium(II) vinylidene complexes [Ru{=C=C(H)R}(η^5 -C₉H₇)(PPh₃)₂][PF₆] [R = Ph (**1**), 4-MeOC₆H₄ (**2**), 4-MeC₆H₄ (**3**), 4-PhC₆H₄ (**4**), 4-FC₆H₄ (**5**), 4-ClC₆H₄ (**6**), 4-IC₆H₄ (**7**), 4-MeCOC₆H₄ (**8**), 4-O₂NC₆H₄ (**9**), ^tBu (**10**), (η^5 -C₅H₄)Fe(η^5 -C₅H₅) (**11**, Fc)] have been synthesized from [RuCl(η^5 -C₉H₇)(PPh₃)₂] and RC≡CH, in a methanolic solution of NaPF₆ at room temperature. The complexes, when dissolved in acetonitrile-*d*₃, release the vinylidene ligand upon thermal activation in the form of the corresponding terminal alkyne, with formation of the solvato complex [Ru(N≡CCD₃)(η^5 -C₉H₇)(PPh₃)₂][PF₆] (**1a**). The reactions, followed by ³¹P{¹H} NMR spectroscopy, exhibit first-order behavior in the vinylidene substrates, and the activation parameters $\Delta H^\ddagger = 24 \pm 1$ kcal mol⁻¹ and $\Delta S^\ddagger = -3 \pm 2$ cal mol⁻¹ K⁻¹ for complex **1** (36–54 °C). The Hammett plot derived from the aryl-substituted complexes yields the reaction parameter $\rho = -1.5$, indicating a rate enhancement effect by electron-donor substituents on the β -C atom. Formation of the vinylidene complex **1** from PhC≡¹³CH as well as release of the alkyne proceeds by an exclusive 1,2 shift of the H atom, as determined by the reactions of [RuCl(η^5 -C₉H₇)(PPh₃)₂] with the ¹³C-labeled alkyne and of the C_α-enriched vinylidene complex [Ru{=¹³C=C(H)Ph}(η^5 -C₉H₇)(PPh₃)₂][PF₆]. The vinylidene moiety undergoes rapid H/D exchange with D₂O/H₂O at room temperature, while the presence of a nitrogen base transforms complex **4** into the corresponding neutral acetylide derivative. The reactions of complexes **4**, **10**, and **11**, performed in solvent mixtures CD₃CN/H(D)₂O, exhibit primary kinetic isotopic effects in the range $k_H/k_D = 1.17$ –1.88, in agreement with an intramolecular 1,2 hydrogen shift mechanism characterized by a nonlinear C–H(D)–C structure of the rate-determining transition state.

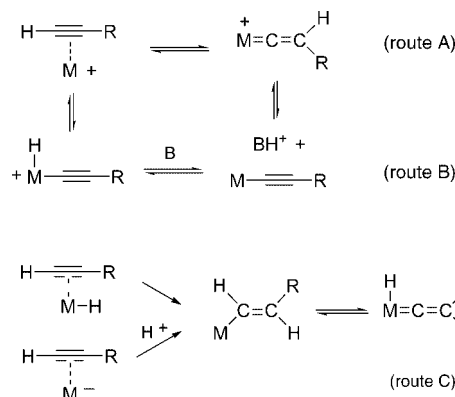
Introduction

Vinylidene ruthenium complexes are active species in organometallic chemistry¹ and in catalysis.² A consequence of the rich and versatile reactivity of vinylidene intermediates is the expansion of the application profile of ruthenium complexes in synthetic organic chemistry.³ Among various synthetic approaches to these species, one direct route involves the isomerization of a metal π -bonded terminal alkyne into the η^1 -vinylidene moiety (Scheme 1).

Scheme 1. η^2 -Alkyne/ η^1 -Vinylidene Isomerization



Scheme 2. Established Reaction Pathways for Alkyne/Vinylidene Isomerization



This apparently simple transformation, which represents a model for organometallic reactions and key steps of catalytic processes, can occur via different pathways, a schematic representation of which is shown in Scheme 2. The η^2 -coordinated alkyne can undergo a 1,2 hydrogen shift over the

* To whom correspondence should be addressed. E-mail: mauro.bassetti@uniroma1.it (M.B.), vcm@uniovi.es (V.C.).

[†] Istituto di Metodologie Chimiche.

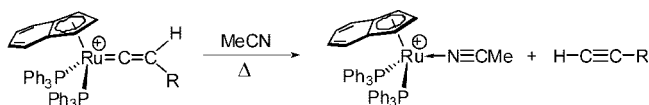
[‡] Universidad de Oviedo.

(1) (a) Bruce, M. I. *Chem. Rev.* **1991**, *91*, 197–257. (b) Puerta, M. C.; Valerga, P. *Coord. Chem. Rev.* **1999**, *193–195*, 977–1025. (c) Wakatsuki, Y. *J. Organomet. Chem.* **2004**, *689*, 4092–4109. (d) Cadierno, V.; Gamasa, M. P.; Gimeno, J. *Coord. Chem. Rev.* **2004**, *248*, 1627–1657.

(2) (a) Naota, T.; Takaya, H.; Murahashi, S.-I. *Chem. Rev.* **1998**, *98*, 2599–2660. (b) Bruneau, C.; Dixneuf, P. H. *Acc. Chem. Res.* **1999**, *32*, 311–323. (c) Dragutan, V.; Dragutan, I. *Platinum Metals Rev.* **2004**, *48*, 148–153. (d) Bruneau, C.; Dixneuf, P. H. *Angew. Chem., Int. Ed.* **2006**, *45*, 2176–2203.

(3) (a) Trost, B. M.; Toste, F. D.; Pinkerton, A. B. *Chem. Rev.* **2001**, *101*, 2067–2096. (b) *Ruthenium in Organic Synthesis*; Murahashi, S.-I., Ed.; Wiley-VCH: Weinheim, Germany, 2004. (c) *Ruthenium Catalysts and Fine Chemistry*; Bruneau, C.; Dixneuf, P. H., Eds.; Springer: Berlin, 2004. (d) Trost, B. M.; Frederiksen, M. U.; Rudd, M. T. *Angew. Chem., Int. Ed.* **2005**, *44*, 6630–6666. (e) Gimeno, J. *Curr. Org. Chem.* **2006**, *10*, 113–225, issue 2 devoted to this topic. (f) Trost, B. M.; McClory, A. *Chem. Asian J.* **2008**, *3*, 164–194.

Scheme 3



C≡C bond (route A),^{4c,5a} or a 1,3 hydrogen shift from a hydridoalkynyl species, proceeding by sequential proton dissociation from ruthenium and protonation at the alkynyl β-C atom (route B).^{4d} Otherwise, in the case of ruthenium hydride complexes, the reaction can proceed by insertion of the alkyne into the Ru–H bond and subsequent rearrangement of the resulting vinyl species into a hydridovinylidene complex, by a hydrogen shift from C_α to ruthenium (route C).^{4e} Various experimental⁴ and theoretical^{4e,g,5} studies analyzed the intimate mechanisms that characterize these reaction pathways, supported by the isolation of some of the corresponding intermediate complexes and by kinetic information.^{4d,6}

The reverse reaction, i.e., the transformation of the vinylidene moiety into the corresponding alkyne, is also a feasible process for ruthenium complexes, accessible in ordinary reaction conditions. In fact, the release of the free alkyne molecule from vinylidene complexes was found to occur in the presence of added nucleophiles.^{6,7} We specifically investigated the utility of this process as a synthetic methodology for the preparation of functionalized terminal alkynes. Upon treatment in acetonitrile under reflux, indenylruthenium(II) vinylidene complexes [Ru{=C=C(H)R}(η⁵-C₉H₇)(PPh₃)₂][PF₆] readily undergo demetalation liberating the corresponding alkyne, with the metal fragment being quantitatively transformed into the cationic solvato complex [Ru(N≡CMe)(η⁵-C₉H₇)(PPh₃)₂][PF₆] (Scheme 3).^{8a} By use of this approach, we synthesized a large variety of terminal γ-ketoalkynes⁹ and 1,4-diyne^{8,10} as well as 1,3-,^{8,11} 1,5-¹² and 1,6-enynes,^{12a} starting from the appropriate vinylidene precursor. This methodology was recently applied to the

preparation of enantiomerically pure terminal alkynes by using the chiral auxiliary [Ru(η⁵-C₉H₇){(R)-BINAP}]⁺.¹³

The conceptual and practical relevance of the η¹-vinylidene to η²-alkyne tautomerization is in contrast with the relatively scarce number of experimental mechanistic studies. The direct access of indenylruthenium(II) vinylidene complexes with different substituents on the β-C atom from the corresponding alkynes and the mild conditions required for their release from the ruthenium center render the process amenable to a detailed mechanistic investigation. In this respect, we now report an experimental study based on kinetic measurements and on the classical tools of physical organic chemistry.

Results and Discussion

Vinylidene Complexes and Reaction Scheme. In this work, the process depicted in Scheme 3 was studied for a series of indenylruthenium(II) vinylidene complexes [Ru{=C=C(H)R}(η⁵-C₉H₇)(PPh₃)₂][PF₆] [R = Ph (**1**), 4-MeOC₆H₄ (**2**), 4-MeC₆H₄ (**3**), 4-PhC₆H₄ (**4**), 4-FC₆H₄ (**5**), 4-ClC₆H₄ (**6**), 4-IC₆H₄ (**7**), 4-MeCOC₆H₄ (**8**), 4-O₂NC₆H₄ (**9**), ⁿBu (**10**), (η⁵-C₅H₅)Fe(η⁵-C₅H₅) (**11**)]. These compounds, which bear alkyl, aryl, and ferrocenyl substituents on the vinylidene moiety, were prepared by reacting a methanolic solution of the chloride precursor [RuCl(η⁵-C₉H₇)(PPh₃)₂] with the corresponding terminal alkyne HC≡CR in the presence of NaPF₆, according to literature procedures (Scheme 4).^{8a,14} The novel derivatives **2–8** and **10**, isolated as air-stable orange solids in 72–92% yield, were characterized by means of standard spectroscopic techniques (IR and ³¹P{¹H}, ¹H, and ¹³C{¹H} NMR), conductance measurements (1:1 electrolytes; Λ_M = 109–119 Ω⁻¹ cm² mol⁻¹), and elemental analyses (details are given in the Experimental Section). The most relevant spectroscopic features are (i) (³¹P{¹H} NMR) the presence of a sole singlet signal (38.05–41.22 ppm), which is consistent with the chemical equivalence of both P atoms, (ii) (¹H NMR) the singlet (**3–5** and **7**) or triplet (**2**, **6**, and **8**, ⁴J_{HP} = 1.6–1.9 Hz; **10**, ³J_{HH} = 7.7 Hz) resonance for the vinylidene proton [Ru]=C=CH at 4.28–5.26 ppm, and (iii) (¹³C{¹H} NMR) the characteristic deshielded signal of the carbenic Ru=C_α, which appears as a triplet (²J_{CP} = 15.7–17.1 Hz) in the range 346.48–353.39 ppm, with C_β resonating as a singlet at higher fields (113.28–118.64 ppm). All of these data are in agreement with those previously reported by us for related indenylruthenium(II) vinylidenes.^{8,12,14,15}

(4) (a) Wakatsuki, Y.; Yamazaki, H.; Kumegawa, N.; Satoh, T.; Satoh, J. Y. *J. Am. Chem. Soc.* **1991**, *113*, 9604–9610. (b) Lompfrey, J. R.; Selegue, J. P. *J. Am. Chem. Soc.* **1992**, *114*, 5518–5523. (c) Wakatsuki, Y.; Koga, N.; Yamazaki, H.; Morokuma, K. *J. Am. Chem. Soc.* **1994**, *116*, 8105–8111. (d) de los Ríos, I.; Tenorio, M. J.; Puerta, M. C.; Valera, P. *J. Am. Chem. Soc.* **1997**, *119*, 6529–6538. (e) Oliván, M.; Clot, E.; Eisenstein, O.; Caulton, K. G. *Organometallics* **1998**, *17*, 3091–3100. (f) García-Yebra, C.; López-Mardomingo, C.; Fajardo, M.; Antiñolo, A.; Otero, A.; Rodríguez, A.; Vallat, A.; Lucas, D.; Mugnier, Y.; Carbó, J. J.; Lledós, A. *Organometallics* **2000**, *19*, 1749–1765. (g) Grotjahn, D. B.; Zeng, X.; Cooksy, A.; Scott Cassel, W.; DiPasquale, A. G.; Zakharov, L. N.; Rheingold, A. L. *Organometallics* **2007**, *26*, 3385–3402.

(5) (a) Silvestre, J.; Hoffmann, R. *Helv. Chim. Acta* **1985**, *68*, 1461–1506. (b) Wakatsuki, Y.; Koga, N.; Werner, H.; Morokuma, K. *J. Am. Chem. Soc.* **1997**, *119*, 360–366. (c) Stegmann, R.; Frenking, G. *Organometallics* **1998**, *17*, 2089–2095. (d) Pérez-Carreño, E.; Paoli, P.; Ienco, A.; Mealli, C. *Eur. J. Inorg. Chem.* **1999**, *131*, 5–1324. (e) Tokunaga, M.; Suzuki, T.; Koga, N.; Fukushima, T.; Horiuchi, A.; Wakatsuki, Y. *J. Am. Chem. Soc.* **2001**, *123*, 11917–11924. (f) De Angelis, F.; Sgamellotti, A.; Re, N. *Organometallics* **2002**, *21*, 5944–5950. (g) De Angelis, F.; Sgamellotti, A.; Re, N. *Dalton Trans.* **2004**, 3225–3230.

(6) Bullock, R. M. *J. Chem. Soc., Chem. Commun.* **1989**, 165–167.

(7) (a) Albertin, G.; Antoniutti, S.; Bordignon, E.; Cazzaro, F.; Ianelli, S.; Pelizzi, G. *Organometallics* **1995**, *14*, 4114–4125. (b) Martin, M.; Gevert, O.; Werner, H. *J. Chem. Soc., Dalton Trans.* **1996**, 2275–2283. (c) Slugovc, C.; Sapunov, V. N.; Wiede, P.; Mereiter, K.; Schmid, R.; Kirchner, K. *J. Chem. Soc., Dalton Trans.* **1997**, 4209–4216. (d) Bruce, M. I.; Hall, B. C.; Tieckink, E. R. T. *Aust. J. Chem.* **1997**, *50*, 1097–1099. (e) Bianchini, C.; Purches, G.; Zanobini, F.; Peruzzini, M. *Inorg. Chim. Acta* **1998**, *272*, 1–3.

(8) (a) Cadierno, V.; Gamasa, M. P.; Gimeno, J.; Pérez-Carreño, E.; García-Granda, S. *Organometallics* **1999**, *18*, 2821–2832. (b) The use of different symmetry restrictions identified an intermediate species between the η²-alkyne and vinylidene complexes and afforded modified values of energy barriers, as described in ref 15.

(9) (a) Cadierno, V.; Conejero, S.; Gamasa, M. P.; Gimeno, J.; Pérez-Carreño, E.; García-Granda, S. *Organometallics* **2001**, *20*, 3175–3189. (b) Cadierno, V.; Conejero, S.; Gamasa, M. P.; Gimeno, J.; Falvello, L. R.; Llusar, R. M. *Organometallics* **2002**, *21*, 3716–3726. (c) Cadierno, V.; Gamasa, M. P.; Gimeno, J.; Pérez-Carreño, E.; García-Granda, S. *J. Organomet. Chem.* **2003**, *670*, 75–83.

(10) Cadierno, V.; Conejero, S.; Gamasa, M. P.; Gimeno, J. *Dalton Trans.* **2003**, 3060–3066.

(11) (a) Cadierno, V.; Gamasa, M. P.; Gimeno, J. *J. Organomet. Chem.* **2001**, *621*, 39–45. (b) Cadierno, V.; Conejero, S.; Gamasa, M. P.; Gimeno, J.; Rodríguez, M. A. *Organometallics* **2002**, *21*, 203–209.

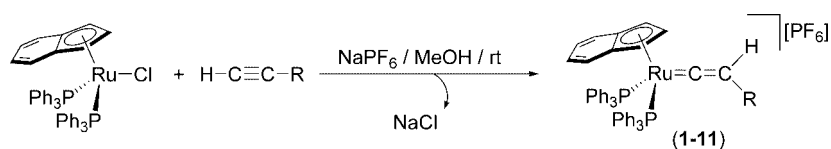
(12) (a) Cadierno, V.; Conejero, S.; Gamasa, M. P.; Gimeno, J. *Organometallics* **2002**, *21*, 3837–3840. (b) Cadierno, V.; Conejero, S.; Díez, J.; Gamasa, M. P.; Gimeno, J.; García-Granda, S. *Chem. Commun.* **2003**, 840–841.

(13) Nishibayashi, Y.; Imajima, H.; Onodera, G.; Uemura, S. *Organometallics* **2005**, *24*, 4106–4109.

(14) (a) Gamasa, M. P.; Gimeno, J.; Martín-Vaca, B. M.; Borge, J.; García-Granda, S.; Pérez-Carreño, E. *Organometallics* **1994**, *13*, 4045–4057. (b) Cadierno, V.; Conejero, S.; Gamasa, M. P.; Gimeno, J.; Asselberghs, I.; Houbrechts, S.; Clays, K.; Persoons, A.; Borge, J.; García-Granda, S. *Organometallics* **1999**, *18*, 582–597.

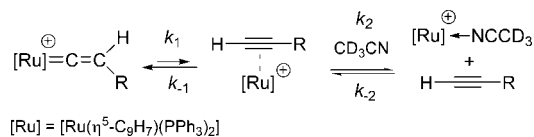
(15) Cadierno, V.; Gamasa, M. P.; Gimeno, J.; González-Bernardo, C.; Pérez-Carreño, E.; García-Granda, S. *Organometallics* **2001**, *20*, 5177–5188.

Scheme 4. Synthesis of Indenylruthenium(II) Vinylidene Complexes



R = Ph (1), 4-MeO-C₆H₄ (2), 4-Me-C₆H₄ (3), 4-Ph-C₆H₄ (4), 4-F-C₆H₄ (5), 4-Cl-C₆H₄ (6), 4-I-C₆H₄ (7), 4-MeCO-C₆H₄ (8), 4-O₂N-C₆H₄ (9), ⁿBu (10), Fc (11)

Scheme 5



In our previous work,^{8a} it was established that the reaction of complex [Ru{=C=C(H)Ph}(η⁵-C₉H₇)(PPh₃)₂][PF₆] (**1**) with CD₃CN can be monitored conveniently by ³¹P{¹H} and ¹H NMR spectroscopy in the temperature range from 20 to 70 °C. The spectra only showed the resonance of the starting material **1** and that assigned to the nitrile complex [Ru(N≡CCD₃)(η⁵-C₉H₇)(PPh₃)₂][PF₆] (**1a**), with the presence of an intermediate π-alkyne species not being observed. This suggested a reaction sequence characterized by an η¹-vinylidene/η²-alkyne equilibrium, although shifted toward the vinylidene, and a rapid displacement of the coordinated alkyne by a solvent molecule, as outlined in Scheme 5.

Ab initio molecular orbital calculations on the η²-alkyne to η¹-vinylidene tautomerization performed on the model complex [Ru(η²-HC≡CH)(η⁵-C₉H₇)(PPh₃)₂]⁺ supported a rate-determining 1,2 hydrogen shift mechanism requiring an energy barrier of 18.9 kcal mol⁻¹, and of 29.9 kcal mol⁻¹ for the reverse process, calculated from the vinylidene rotamer of highest energy.^{8b} This latter value is low enough to be overcome under the experimental reaction conditions, allowing the transformation of the thermodynamically more stable η¹-vinylidene complex into the labile η²-alkyne intermediate, in which the coordinated alkyne molecule is rapidly exchanged by acetonitrile. The occurrence of the η¹-vinylidene/η²-alkyne tautomerism was well established in the case of the more electrophilic carbonyl complexes [RuX(η⁵-1,2,3-R₃C₉H₄)(CO)(PR₃)], which reacted with terminal alkynes, giving equilibrium mixtures of observable η¹-vinylidene and η²-alkyne isomers [Ru{=C=C(H)R'}(η⁵-1,2,3-R₃C₉H₄)(CO)(PR₃)][BF₄] and [Ru(η²-HC≡CR')(η⁵-1,2,3-R₃C₉H₄)(CO)(PR₃)][BF₄] (X = Br, R = Me, PR₃ = PⁱPr₃, PPh₃; X = I, R = H, PR₃ = PⁱPr₃).¹⁵

Kinetic and Thermodynamic Analysis. The reactions of complexes **1–11** in neat CD₃CN or in the solvent mixture CD₃CN/THF were followed by ³¹P{¹H} NMR between 36 and 54 °C, by monitoring the disappearance of the starting vinylidene complex and the formation of the corresponding nitrile derivative **1a**. The analysis of the exponential decay of the signal intensities of the compounds or of the corresponding integrated values, according to the first-order rate equation, gave the values of the observed rate constants, *k*_{obs}. The first-order fittings improved significantly in the presence of approximately equimolar amounts of P(*o*-tolyl)₃, used as an internal standard, or of excess PPh₃ with respect to **1–11**, suggesting that dissociation of phosphine is implicated in decomposition pathways rather than along the reaction coordinate of the vinylidene/alkyne transformation. The *k*_{obs} values calculated from the disappearance of the starting material were within experimental error of those obtained for the formation of the acetonitrile product, as

exemplified in Figure 1 for the reaction of complex **5**. This is yet another piece of evidence consistent with the hypothesis that the π-alkyne intermediate species depicted in Scheme 5 is formed under transient conditions and either returns rapidly to the vinylidene complex or is captured by solvent to yield the acetonitrile adduct and the alkyne.

By application of the steady-state approximation to the η²-alkyne complex and assuming the *k*₋₂ term to be negligible, the following rate equation is derived (eq 1):

$$k_{\text{obs}} = k_1 k_2 [\text{CD}_3\text{CN}] / (k_{-1} + k_2 [\text{CD}_3\text{CN}]) \quad (1)$$

Because of the lability of the π-alkyne adduct toward displacement by a solvent and an excess of acetonitrile, it occurs that *k*₂[CD₃CN] ≫ *k*₋₁, so that eq 1 reduces to eq 2.

$$k_{\text{obs}} = k_1 \quad (2)$$

The *k*_{obs} values derived from the disappearance of the substrates can therefore be regarded as associated with the first-order and rate-determining transformation of the vinylidene complex into the η²-alkyne intermediate (*k*₁, Scheme 5). Values of *k*_{obs} are reported in Table 1 for the various substrates and conditions. The experiments carried out in the solvent mixture CD₃CN/THF do not show an appreciable rate dependence on the nitrile within the accessible concentration range (entries 1–3), corresponding to zero-order behavior on the reagent and thus indicating its involvement in the second step of the reaction.

The reversibility of the η¹-vinylidene/η²-alkyne isomerism was checked by performing the reaction of complex **1** in the absence and presence of free PhC≡CH (0.72 M), under comparable conditions: after 6.5 h at 44.5 °C, the integral ratios of **1a** vs **1** were 7.5, corresponding to 88% of the reaction, and 2.0, corresponding to 66% of the reaction, respectively. While in the absence of free alkyne the starting material disappeared

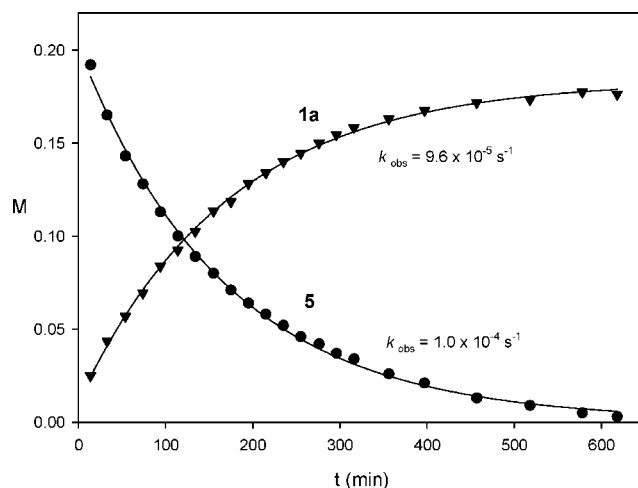


Figure 1. Plots of concentration vs time from the reaction of complex **5** (47 °C in neat CD₃CN) and corresponding first-order fits of the substrate disappearance ($-d[\mathbf{5}]/dt = 1.0 \times 10^{-4} \text{ s}^{-1}$) and product formation ($d[\mathbf{1a}]/dt = 9.6 \times 10^{-5} \text{ s}^{-1}$).

Table 1. Values of Observed Rate Constants, $-d[1-11]/dt$ (k_{obs}), for the Reactions of Complexes $[\text{Ru}\{\text{C}=\text{C}(\text{H})\text{R}\}(\eta^5\text{-C}_9\text{H}_7)(\text{PPh}_3)_2][\text{PF}_6]$ (1–11) with CD_3CN ^{a,b}

entry	substrate, R	CD_3CN , M	t , °C	$k_{\text{obs}} \times 10^4$, s ⁻¹
1	1, Ph	1.19 ^c	49	4.0
2	1, Ph	1.91 ^c	49	4.5
3	1, Ph	2.89 ^c	49	4.1
4	1, Ph	neat	36	0.4
5	1, Ph	neat	40	0.7
6	1, Ph	neat	47	1.6
7	1, Ph	neat	54	3.5
8	2, 4-MeOC ₆ H ₄	neat	47	4.2
9	3, 4-MeC ₆ H ₄	neat	47	2.0
10 ^d	3, 4-MeC ₆ H ₄	neat	47	2.1
11	4, 4-PhC ₆ H ₄	neat	47	0.97
12	5, 4-FC ₆ H ₄	neat	47	1.00
13	5- <i>d</i> ^e , 4-FC ₆ H ₄	neat	47	1.04
14	6, 4-ClC ₆ H ₄	neat	47	0.50
15	7, 4-IC ₆ H ₄	neat	47	0.42
16	8, 4-MeCOC ₆ H ₄	neat	47	0.17
17	9, 4-O ₂ NC ₆ H ₄	neat	47	0.10
18	10, ⁿ Bu	neat	47	4.9
19	11, Fc	neat	47	2.4

^aThe measurements are reproducible within 10%. ^b[1–11] = 0.018–0.028 M. ^cIn THF. ^dIn the presence of PPh₃ (0.081 M). ^e5-*d* is $[\text{Ru}\{\text{C}=\text{C}(\text{D})\text{-4-FC}_6\text{H}_4\}(\eta^5\text{-C}_9\text{H}_7)(\text{PPh}_3)_2][\text{PF}_6]$ (details on its preparation are given in the Experimental Section).

at longer reaction times, with the reaction still being in progress at $t = 6.5$ h, the relative intensities of the acetonitrile adduct to the η^1 -vinylidene complex did not show further changes in the presence of added phenylacetylene, indicating the attainment of an equilibrium mixture. The values of equilibrium constant $K = 0.082$ and standard free energy $\Delta G^\circ = 1.6$ kcal mol⁻¹ at 44.5 °C were calculated from the molar concentration data of the species in eq 3. These experimental thermodynamic parameters show that the equilibrium (Scheme 5 and eq 3) is still shifted to the left even when the η^2 -1-alkyne species is transformed into the corresponding acetonitrile derivative. The values apparently contrast with the theoretical calculations performed on the models $[\text{Ru}\{\text{C}=\text{C}(\text{H})\text{Me}\}(\eta^5\text{-C}_5\text{H}_5)(\text{PMe}_3)_2][\text{PF}_6]$ and $[\text{Ru}(\eta^2\text{-HC}\equiv\text{CH})(\eta^5\text{-C}_9\text{H}_7)(\text{PPh}_3)_2]^+$,^{8,15} which show that the η^1 -vinylidene complex is thermodynamically more stable than the η^2 -1-alkyne species by about 12 kcal mol⁻¹. Besides the different structure and medium between the theoretical calculations (gas phase) and this experimental evaluation, the smaller free energy value found for the equilibrium in eq 3 can be ascribed to the greater stability of the solvato complex with respect to the η^2 -1-alkyne adduct.



It occurs that the stability of **1a** and the large molar excess of acetonitrile in the synthetic and kinetic experiments drive the reactions toward completion in the absence of added alkyne.

Migratory Aptitude of H vs Ph. Because the most common migrating species in the vinylidene/alkyne isomerizations is hydrogen, the majority of the theoretical studies were carried out on the parent acetylene complexes, thus avoiding any ambiguity arising from competitive migratory aptitudes of the two groups linked to the triple bond. However, the alkyne-to-vinylidene reaction can also occur by migration of SiR₃,¹⁶ SnPh₃,¹⁷ SME,¹⁸ or iodine.^{1c,19} It is also worth noting that a larger migratory aptitude of Ph vs Me was observed in the

irreversible vinylidene to η^2 -alkyne isomerization in complex $[\text{Fe}\{\text{C}=\text{C}(\text{Me})\text{Ph}\}(\eta^5\text{-C}_5\text{H}_5)(\text{CO})_2]^+$.²⁰ With these precedents in mind and taking into account that aryl groups are known to undergo 1,2 shifts between adjacent carbons in various organic substrates,²¹ we regarded as essential, in light of a proper interpretation of the kinetic data and of the implications on the mechanism of the vinylidene/alkyne isomerization, to identify experimentally the migrating group in both the forward and reverse steps of the tautomerization process. To this end, $\text{PhC}\equiv\text{C}^{13}\text{CH}$ was reacted with $[\text{RuCl}(\eta^5\text{-C}_9\text{H}_7)(\text{PPh}_3)_2]$ in the presence of NaPF₆ and, as assessed by ¹³C{¹H} NMR spectroscopy, yielded solely the C_α-enriched vinylidene complex $[\text{Ru}\{\text{C}=\text{C}(\text{H})\text{Ph}\}(\eta^5\text{-C}_9\text{H}_7)(\text{PPh}_3)_2][\text{PF}_6]$ (**1b**), by exclusive migration of the H atom (see the Experimental Section and the Supporting Information for details). In addition, starting from this vinylidene complex, the free alkyne $\text{PhC}\equiv\text{C}^{13}\text{CH}$ was subsequently released by reaction with CD₃CN (50 °C, 7 h).²² These experiments represent the first experimental evidence for the larger migratory aptitude of H vs Ph in both the alkyne-to-vinylidene and vinylidene-to-alkyne transformations.

Activation Parameters and Hammett Plot. The experiments carried out on complex **1** at different temperatures and the derived Eyring plot yielded values of $\Delta H^\ddagger = 24 \pm 1$ kcal mol⁻¹ and $\Delta S^\ddagger = -3 \pm 2$ cal mol⁻¹ K⁻¹. These activation parameters can be compared with those obtained for the ruthenium complex $[\text{Ru}\{\text{C}=\text{C}(\text{H})\text{Me}\}(\eta^5\text{-C}_5\text{H}_5)(\text{PMe}_3)_2][\text{PF}_6]$ in acetonitrile (80–110 °C, $\Delta H^\ddagger = 27$ kcal mol⁻¹ and $\Delta S^\ddagger = -5$ cal mol⁻¹ K⁻¹)⁶ and for the molybdenum complex $[\text{Mo}\{\text{C}=\text{C}(\text{H})\text{Bu}\}(\eta^5\text{-C}_5\text{H}_5)(\text{CO})(\text{NO})]$ in toluene-*d*₈ (80–140 °C, $\Delta H^\ddagger = 29$ kcal mol⁻¹ and $\Delta S^\ddagger = -2$ cal mol⁻¹ K⁻¹),²³ with both processes occurring via migration of hydrogen and displaying similar values of ΔS^\ddagger . The activation entropy close to zero rules out the occurrence of either associative or dissociative mechanisms and suggests a unimolecular isomerization process of least motion for the rate-determining step of the reaction.²⁴

The decreased reactivity exhibited by the 4-nitrophenyl-substituted vinylidene complex **9** versus that of ferrocenyl complex **11** in acetonitrile at reflux had shown that the process is favored by electron-releasing substituents on the vinylidene group.^{8a} The kinetic experiments here performed on the series of aryl complexes with para substituents ranging from methoxy to the nitro groups yielded the Hammett plot shown in Figure 2, from the corresponding k_{obs} and σ_{p} values.²¹ The plot gives a linear fit, indicating that there are no changes in the mechanism upon variation of the electronic properties of the substituents. The derived ρ value, -1.5 , confirms the accelerating effect by

(19) (a) Löwe, C.; Hund, H. U.; Berke, H. *J. Organomet. Chem.* **1989**, *371*, 311–325. (b) Miura, T.; Iwasawa, N. *J. Am. Chem. Soc.* **2002**, *124*, 518–519.

(20) Bly, R. S.; Zhong, Z.; Kane, C.; Bly, R. K. *Organometallics* **1994**, *13*, 899–905.

(21) Smith, M. B.; March, J. *March's Advanced Organic Chemistry: Reactions, Mechanisms, and Structure*, 5th ed.; John Wiley & Sons, Inc.: New York, 2001.

(22) This was confirmed by a comparison of the ¹H and ¹³C{¹H} NMR data with those of the commercially available $\text{PhC}\equiv\text{C}^{13}\text{CH}$ (see the Supporting Information).

(23) Ipaktschi, J.; Mohsseni-Ala, J.; Uhlig, S. *Eur. J. Inorg. Chem.* **2003**, *431*, 3–4320.

(24) (a) The phosphine substitution reactions proceeding by a dissociative mechanism in complexes $[\text{RuCl}(\eta^5\text{-L})(\text{PPh}_3)_2]$ exhibited positive values of $\Delta S^\ddagger = 11 \pm 2$ (L = C₆H₇) and 17 ± 2 (L = C₅H₅) cal mol⁻¹ K⁻¹. Gamasa, M. P.; Gimeno, J.; Gonzales-Bernardo, C.; Martín-Vaca, B. M.; Monti, D.; Bassetti, M. *Organometallics* **1996**, *15*, 302–308. (b) A rate-determining phosphine dissociative step can be further excluded from the lack of rate-retarding effects upon performance of the reaction of complex **3** in the presence of added PPh₃ (Table 1, entries 9 and 10) or of complex **1** in CD₃CN/THF up to $[\text{PPh}_3] = 0.45$ M.

(16) (a) Sakurai, H.; Fujii, T.; Sakamoto, K. *Chem. Lett.* **1992**, 339–342. (b) Werner, H.; Lass, R. W.; Gevert, O.; Wolf, J. *Organometallics* **1997**, *16*, 4077–4088. (c) Foerster, J.; Kakoschke, A.; Goddard, R.; Rust, J.; Warchow, R.; Butenschön, H. *J. Organomet. Chem.* **2001**, *617*–*618*, 412–422.

(17) Baum, M.; Mahr, N.; Werner, H. *Chem. Ber.* **1994**, *127*, 1877–1886.

(18) Miller, D. C.; Angelici, R. J. *Organometallics* **1991**, *10*, 79–89.

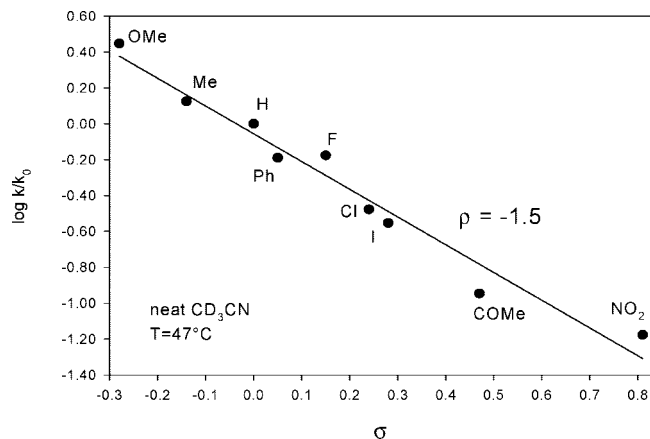


Figure 2. Hammett plot for the reactions of para-substituted arylvinylidene complexes $[\text{Ru}\{\text{=C=C(H)}(4\text{-X-C}_6\text{H}_4)\}(\eta^5\text{-C}_9\text{H}_7\text{-PPh}_3)_2][\text{PF}_6]$ in acetonitrile- d_3 .

electron donation and indicates substantial development of positive charge, or dissipation of the electron density, in the transition state of the rate-determining step. The reactivities displayed by compounds **10** and **11** are in agreement with the electron-donor character of the *n*-butyl and ferrocenyl moieties (Table 1, entries 18 and 19).

Kinetic Isotopic Effect (KIE). KIEs are largely employed as fine tools for the identification of the rate-limiting step and the symmetry of the related activated complex.²¹ In the case of $[\text{Mo}\{\text{=C=C(H)Bu}\}(\eta^5\text{-C}_5\text{H}_5)(\text{CO})(\text{NO})]$ and $[\text{W}\{\text{=C=C(H)R}\}(\eta^5\text{-C}_5\text{H}_5)(\text{CO})(\text{NO})]$ ($\text{R} = \text{SiMe}_2\text{Bu}$, SiMePh_2 , Bu) complexes, migratory aptitudes and different reaction pathways were proposed for the η^1 -vinylidene to η^2 -alkyne transformation on the basis of primary and secondary KIEs, which were found to span in the interval $k_{\text{H}}/k_{\text{D}} = 1.2\text{--}15.7$.^{23,25} The rate constants for the reactions of complexes $[\text{Ru}\{\text{=C=C(D)}(4\text{-FC}_6\text{H}_4)\}(\eta^5\text{-C}_9\text{H}_7)(\text{PPh}_3)_2][\text{PF}_6]$ (**5-d**) and $[\text{Ru}\{\text{=C=C(H)}(4\text{-FC}_6\text{H}_4)\}(\eta^5\text{-C}_9\text{H}_7)(\text{PPh}_3)_2][\text{PF}_6]$ (**5**) apparently showed the same values (Table 1, entries 12 and 13), thus giving no evidence of rate dependence on the nature of the migrating hydrogen isotope. The lack of an isotopic effect would suggest that hydrogen migration does not occur in the rate-limiting step; nevertheless, the migratory aptitude of H vs Ph determined with the ^{13}C -labeled compounds ruled out any competition with migration of the aryl group. This apparent controversy prompted us to take into proper account the nature of the vinylidene moiety and to investigate further its behavior under the conditions of the kinetic experiments. In particular, we investigated the occurrence of acid–base exchange processes, which may arise from the acidic character of the $\beta\text{-H}$.^{26,27} The addition of excess D_2O to the complexes in acetonitrile- d_3 solutions caused the disappearance of the ^1H NMR signal of the $\text{Ru}=\text{C}=\text{CHAr}^+$

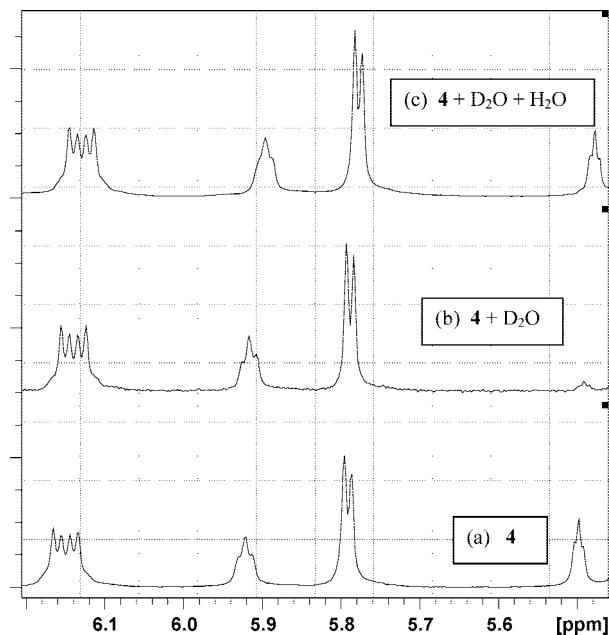


Figure 3. ^1H NMR spectra of complex **4** (0.019 M) (a), after the addition of D_2O (10 μL , 1.07 M) (b), and further addition of H_2O (25 μL , 2.6 M) (c), in acetonitrile- d_3 at room temperature.

group at 5.45 (**2**), 5.51 (**4**), 5.46 (**5**), 5.45 (**6**), and 5.48 (**8**) ppm, within the time of mixing at room temperature. Figure 3 shows the ^1H NMR spectra of complex **4** in acetonitrile- d_3 (a) after the addition of an excess of D_2O (b). The proton resonance of the vinylidene group is readily restored upon subsequent addition of H_2O (c). This H/D exchange process presumably occurs via a dissociative mechanism, as observed in the case of complexes $[\text{Mo}\{\text{=C=C(H)Bu}\}(\eta^5\text{-C}_5\text{H}_5)(\text{CO})(\text{NO})]$ and $[\text{W}\{\text{=C=C(H)SiMe}_2\text{Bu}\}(\eta^5\text{-C}_5\text{H}_5)(\text{CO})(\text{NO})]$,²³ and in agreement with the rapid and irreversible formation of the acetylide derivative upon treatment of complex **4** with Et_3N or with the sterically hindered Hünig base.²⁸

These facts indicate a rapid exchange of the vinylidene hydrogen or deuterium with water, due to remarkable kinetic acidity, and imply that the presence of trace moisture in the acetonitrile- d_3 solvent may have severely affected the kinetic measurement of complex **5-d**. A second implication is that the desired deuterated vinylidene derivative can be obtained in situ and buffered against isotopic scrambling by maintaining an excess of the isotope donor. Therefore, kinetic experiments were performed in the presence of an excess of either D_2O or H_2O . The results obtained for three pairs of experiments are shown in Table 2.

These values of $k_{\text{H}}/k_{\text{D}}$ ratios are typical of primary KIEs exhibited in 1,2 hydrogen migrations over C–C bonds, usually in the range 1–2.^{21,29} The small values compared to those generally observed in intermolecular reactions are due to the nonlinear geometry of the three-center C–H(D)–C transition

(25) In spite of its obvious significance for these processes characterized by hydrogen migration, this parameter was not evaluated in previous studies regarding ruthenium complexes, except for the case of the 1,3 hydrogen shift mechanism from hydrido/alkynyl complexes.^{4d}

(26) (a) Davison, A.; Selegue, J. P. *J. Am. Chem. Soc.* **1978**, *100*, 7763–7765. (b) Bruce, M. I.; Wallis, R. C. *Aust. J. Chem.* **1979**, *32*, 1471–1485. (c) Bruce, M. I.; Wong, F. S.; Skelton, B. W.; White, A. H. *J. Chem. Soc., Dalton Trans.* **1982**, 2203–2207. (d) Ipaktschi, J.; Mohsseni-Ala, J.; Dülmer, A.; Loschen, C.; Frenking, G. *Organometallics* **2005**, *24*, 977–989.

(27) Wakatsuki specifically pointed out that the occurrence of deprotonation/protonation processes for the pathways depicted in Scheme 2 should be taken into account, especially for reactions in protic solvents.^{1c} In this respect, the isomerization of complex $[\text{Mo}\{\text{=C=C(H)Bu}\}(\eta^5\text{-C}_5\text{H}_5)(\text{CO})(\text{NO})]$ proceeded to completion in refluxing toluene after 24 h, in refluxing ethanol after 2 h, and in THF with 10% aqueous NaOH after 20 min at room temperature.²³

(28) The addition of excess Et_3N or $\text{Et}^t\text{Pr}_2\text{N}$ to a solution of complex **4** in acetonitrile caused immediate and quantitative formation of a yellow precipitate, which displayed only one $^{31}\text{P}\{^1\text{H}\}$ NMR resonance, at δ 51.55 ppm (CD_2Cl_2), and the IR stretching band $\nu_{\text{C}=\text{C}}$ at 2074 cm^{-1} (CH_2Cl_2 , strong), in agreement with the structure of a σ -acetylide complex.^{14,15} On the other hand, the addition of excess HBF_4 to complex **4** in CD_3CN caused no changes in the $^{31}\text{P}\{^1\text{H}\}$ NMR spectrum after 1 h at room temperature.

(29) In principle, a secondary KIE cannot be excluded. A case of this type was found in the vinylidene-to-alkyne isomerization of complex $[\text{W}\{\text{=C=C(H)Si}(\text{Me})_3\}(\eta^5\text{-C}_5\text{H}_5)(\text{CO})(\text{NO})]$ ($k_{\text{H}}/k_{\text{D}} = 1.20$, 130–150 °C in toluene- d_8), proposed to proceed by preferred migration of the silyl group versus hydrogen.²³

Table 2. Values of Observed Rate Constants for the Isomerization Reactions of Complexes $[\text{Ru}\{\text{C}=\text{C}(\text{H})\text{R}\}(\eta^5\text{-C}_9\text{H}_7)(\text{PPh}_3)_2][\text{PF}_6]^a$ ($\text{R} = p\text{-PhC}_6\text{H}_4$, ^nBu , Fc) in Aqueous (H_2O or D_2O) Acetonitrile- d_3 Solutions, in the Presence of PPh_3^b

entry	substrate, R	$[\text{H}_2\text{O}]$, M	$[\text{D}_2\text{O}]$, M	t , °C	k_{obs} , s^{-1}	$k_{\text{H}}/k_{\text{D}}$
1	4 , $p\text{-PhC}_6\text{H}_4$	2.13		49.5	$9.8 (\pm 0.4) \times 10^{-5}$	1.17
2	4 , $p\text{-PhC}_6\text{H}_4$		2.11	49.5	$8.4 (\pm 0.4) \times 10^{-5}$	
3	10 , ^nBu	4.19		38.2	$1.6 (\pm 0.1) \times 10^{-4}$	1.88
4	10 , ^nBu		4.17	38.2	$8.5 (\pm 0.6) \times 10^{-5}$	
5	11 , Fc	2.64		45.2	$3.1 (\pm 0.2) \times 10^{-4}$	1.19
6	11 , Fc		2.61	45.2	$2.6 (\pm 0.1) \times 10^{-4}$	

^a 0.022–0.034 M. ^b 0.025–0.027 M.

states and result from compensating effects in the bending and stretching vibrations.³⁰ A similar case was found for the molybdenum complex $[\text{Mo}\{\text{C}=\text{C}(\text{H})^i\text{Bu}\}(\eta^5\text{-C}_5\text{H}_5)(\text{CO})(\text{NO})]$ (in toluene- d_8 , 80–140 °C) undergoing hydrogen shift in the rate-determining step and exhibiting $k_{\text{H}}/k_{\text{D}} = 2.0 \pm 0.2$.²³ There are no significant rate changes in the aqueous solvent mixtures with respect to neat acetonitrile, suggesting that an intermolecular process characterized by stepwise proton dissociation from C_β and proton attack to C_α can be reasonably excluded (route B, Scheme 2), in agreement with the different reaction of complex **4** in the presence of a nitrogen base.²⁸ This case was found for the vinylidene/alkyne isomerization of complex $[\text{Mo}\{\text{C}=\text{C}(\text{H})^i\text{Bu}\}(\eta^5\text{-C}_5\text{H}_5)(\text{CO})(\text{NO})]$ performed in ethanol- d_6 , as supported by the large values of isotopic effects ($k_{\text{H}}/k_{\text{D}} = 7\text{--}16$) accounting for bimolecular transition states with symmetric and linear $\text{C}_\beta\text{---H}(\text{D})\text{---O}$ structures (O = oxygen of the proton acceptor ethanol).²³

Mechanism of the Reaction. Various experimental evidences of this work, specifically reaction order, entropy of activation, absolute value of the reaction parameter $\rho > 1$, KIE, and the absence of rate depression in the presence of free phosphine indicate that the rearrangement of the $\text{C}=\text{CHR}$ group is the slowest step along the transformation of the vinylidene complexes into the solvato complex **1a** in Scheme 5.³¹ This fact can be regarded as fortunate, in that the derived information bears directly on the mechanism of the vinylidene to η^2 -alkyne rearrangement because of the transient character of the π -alkyne species. The discussion of our experimental findings will focus on the reaction pathway outlined in route A of Scheme 2. In fact, it is well documented by experimental^{4b} and theoretical^{4c,5e,f,8,15} information that the most common pathway accounting for the alkyne/vinylidene isomerization mediated by ruthenium(II) complexes proceeds via a direct 1,2 hydrogen shift. Pathway C is peculiar of hydrido complexes, while pathway B, involving the formation of high-energy hydridoalkynyl intermediates, was proven to be accessible in the chemistry of Co,³² Rh,^{4g} and Ir³³ and in the specific case of the electron-rich ruthenium systems of type $[\text{Ru}(\eta^5\text{-C}_5\text{Me}_5)(\text{P})_2]^+$ [$\text{P}_2 = 1,2\text{-bis}(\text{diisopropylphosphino})\text{ethane}$, 2PEt_3].^{4d,34}

Following from the seminal work of Silvestre and Hoffmann on the intimate mechanisms of the η^2 -alkyne/ η^1 -vinylidene isomerization performed at the extended Hückel level for the

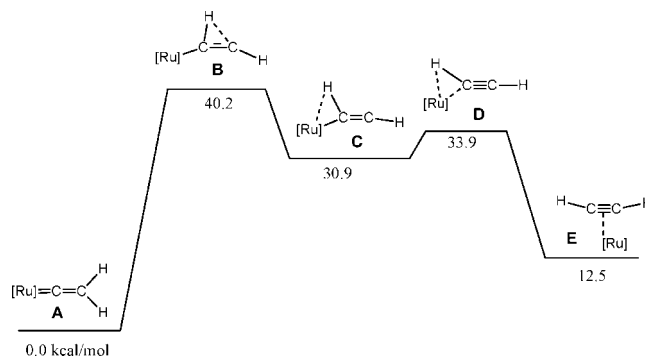


Figure 4. Energy diagram calculated for the metal fragment $[\text{Ru}(\eta^5\text{-C}_9\text{H}_7)(\text{PH}_3)_2]^+$ ($[\text{Ru}]$), as adopted from ref 15 for the transformation of the vinylidene into the π -alkyne species (the origin is fixed at 0.0 kcal mol⁻¹ in the vinylidene complex).

d^6 metal fragment $\text{Mn}^{1,5a}$ various theoretical studies, mainly density functional theory calculations, were performed during the past few years using half-sandwich isoelectronic metal fragments of Ru^{II} , such as $[\text{Ru}(\eta^5\text{-Cp})(\text{PH}_3)_2]^+$,^{5e} $[\text{Ru}(\eta^5\text{-Cp})(\text{PMe}_3)_2]^+$,^{5f} and $[\text{Ru}(\eta^5\text{-Ind})(\text{PH}_3)\text{L}]^+$ (L = PH_3 , CO).^{8,15} With regard to the latter case (L = PH_3), which is the model of the complexes used in the present kinetic studies, calculated structures of various intermediates and transition states involved in the isomerization of the $\eta^1\text{-C}=\text{CH}_2/\eta^2\text{-HC}\equiv\text{CH}$ systems were reported.¹⁵ Figure 4 shows the energy profile ordered from η^1 -vinylidene to η^2 -alkyne with an energy barrier estimated as 40.2 kcal mol⁻¹. This is associated with hydrogen migration from the C_β to C_α atoms of the vinylidene group, yielding an η^2 -(C–H) intermediate (C). The slippage of the ruthenium center over the C2 fragment via a second transition state of lower energy (D) produces the final η^2 -alkyne complex E. The observation of this energy diagram points out to the occurrence of a late transition state, in which the structure of the activated complex B resembles that of the intermediate C rather than that of the starting vinylidene complex A.

In the analysis of the kinetic information with respect to the mechanism outlined in Figure 4, the implicit differences between computational and experimental conditions should be taken into account. For instance, the experimental value of the activation enthalpy exhibited by complex **1** (24 kcal mol⁻¹) indicates consistent stabilization of the intermediate and activated complex by solvent, vinylidene substituents, and/or ligands in the real system. The charge distribution in the cationic substrate, in the π -alkyne complex, and most so along the reaction coordinate plays an important role during the process, as pointed out by the fact that the reaction proceeds in the highly polar solvent acetonitrile. The vinylidene moiety is regarded as a π acceptor with respect to the corresponding η^2 -alkyne, being in fact stabilized by electron-rich metal fragments via back-donation from filled metal d orbitals to an empty π orbital of the vinylidene ligand.^{1,2,5g} Thus, electron-withdrawing substituents favor this interaction and render the vinylidene complex more inert toward the isomerization, as shown by the reduced k_{obs} values of the related complexes with respect to the phenyl derivative **1** (Table 2). The overall electronic influence on the reaction rate may be a combination of effects on both the ground and transition states. In fact, the electronic effect on the reaction rate represented by the value of the reaction parameter $\rho = -1.5$ indicates increasing carbocation character acquired by C_β during the process, as a result of $\text{C}_\beta\text{---H}$ bond breaking, and corresponding lowering of the transition state energy promoted by

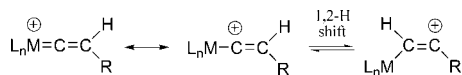
(30) More O'Ferrall, R. A. *J. Chem. Soc., B* **1970**, 78, 5–790, and references cited therein.

(31) The slow attack of acetonitrile assisted by indenyl ring slippage would correspond to a second-order reaction and negative entropy of activation.

(32) Bianchini, C.; Peruzzini, M.; Vacca, A.; Zanolini, F. *Organometallics* **1991**, 10, 3697–3707.

(33) (a) García-Alonso, F. J.; Höhn, H.; Wolf, J.; Otto, H.; Werner, H. *Angew. Chem., Int. Ed. Engl.* **1985**, 24, 406–408. (b) Schaefer, M.; Wolf, J.; Werner, H. *Organometallics* **2004**, 23, 5713–5728.

(34) Bustelo, E.; Carbó, J. J.; Lledós, A.; Mereiter, K.; Puerta, M. C.; Valerga, P. *J. Am. Chem. Soc.* **2003**, 125, 3311–3321.

Scheme 6. Lewis Structures of a Cationic Vinylidene Complex Involved in Hydrogen Migration^{5a}


electron-releasing substituents (Scheme 6).³⁵ This analysis is in agreement with the late character of the transition state **B**, in which the C_α–H bond is significantly formed compared with the long C_β–H distance (1.66 Å).¹⁵

The Hückel analysis in the Mn^I fragment indicated that the hydrogen migration can be regarded as protonic.^{5a} Later, in the course of the molecular orbital calculations performed on the neutral system [RuCl₂(PH₃)₂],^{4c} it was inferred that “the migrating hydrogen behaves as a naked proton rather than a hydride”. In our opinion, the substituent effect and the charge distribution in the starting vinylidene complex (Scheme 6) may imply that the hydrogen migrates as a hydride toward the electron-deficient C_α, in analogy with rearrangements in organic substrates.²¹ In fact, a rate-enhancing effect by electron-donor substituents would not support proton migration in the rate-limiting step because of the resulting destabilization of the residual electron pair. Probably, this point may need further analysis by theoretical investigations.

The values of the *k_H/k_D* ratios point out to a primary KIE and identify the hydrogen migrating over the C–C bond, in line with the intramolecular nature of the 1,2 hydrogen shift. Among the various convergent data arising from synthetic, kinetic, and computational studies, the KIEs here observed can be regarded as the most supportive experimental evidence of the mechanism depicted in Figure 4, in agreement with a three-center structure of the transition state (**B**; Figure 4).

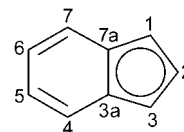
Conclusions

The rate measurements of the release of terminal alkynes from indenylruthenium(II) complexes, [Ru{=C=C(H)R}(η⁵-C₉H₇)(PPh₃)₂][PF₆], affording the nitrile solvato complex **1a**, represent an excellent source of experimental data regarding the mechanism of isomerization of the η¹-β-substituted vinylidene moiety into the labile η²-π-alkyne complex. The kinetic acidity of the vinylidene β-hydrogen induces rapid H/D exchange at room temperature in the presence of D₂O/H₂O, while a neutral alkynyl complex is formed in the presence of a nitrogen base. The use of ¹³C-labeled compounds reveals the larger migratory aptitude of H vs Ph in both vinylidene formation and the release of free alkyne. β-Substituent electronic effects and KIEs on the Ru(=C=CHR)⁺/Ru(η²-HC≡CR)⁺ transformation support an intramolecular 1,2 hydrogen shift mechanism, in substantial agreement with the mechanistic pathway previously postulated from theoretical calculations on the indenylruthenium(II) models of the reaction.^{8,15}

Experimental Section

Synthetic procedures were performed under an atmosphere of dry nitrogen using vacuum-line and standard Schlenk techniques. Solvents were dried by standard methods and distilled under nitrogen before use. All reagents were obtained from commercial suppliers and used without further purification with the exception

of complexes [RuCl(η⁵-C₉H₇)(PPh₃)₂]³⁶ and [Ru{=C=C(H)R}(η⁵-C₉H₇)(PPh₃)₂][PF₆] [R = Ph (**1**),^{14a} 4-O₂NC₆H₄ (**9**),^{14b} and Fc (**11**)⁸] and the terminal alkynes 1-iodo-4-ethynylbenzene³⁷ and 4-ethynylacetophenone.³⁸ IR spectra were recorded on a Perkin-Elmer 1720-XFT spectrometer. The conductivities were measured at room temperature, in ca. 10⁻³ mol dm⁻³ acetone solutions, with a Jenway PCM3 conductimeter. The C and H analyses were carried out with a Perkin-Elmer 2400 microanalyzer. NMR spectra were recorded on a Bruker DPX300 instrument at 300 MHz (¹H), 121.5 MHz (³¹P), or 75.4 MHz (¹³C), using SiMe₄ or 85% H₃PO₄ as standards. DEPT experiments have been carried out for all of the compounds reported in this paper. The numbering for the indenyl skeleton is as follows:



Synthesis of [Ru{=C=C(H)R}(η⁵-C₉H₇)(PPh₃)₂][PF₆] [R = 4-MeOC₆H₄ (2**), 4-MeC₆H₄ (**3**), 4-PhC₆H₄ (**4**), 4-FC₆H₄ (**5**), 4-ClC₆H₄ (**6**), 4-IC₆H₄ (**7**), 4-MeCOC₆H₄ (**8**), and ^tBu (**10**)].**

General Procedure. A solution of [RuCl(η⁵-C₉H₇)(PPh₃)₂] (500 mg, 0.65 mmol), NaPF₆ (220 mg, 1.3 mmol), and the appropriate terminal alkyne (1.3 mmol) in 50 mL of methanol was stirred at room temperature for 4 h. The solvent was then removed under vacuum, the crude product extracted with dichloromethane (ca. 20 mL), and the extract filtered over Kieselguhr. Concentration of the resulting solution (ca. 5 mL) followed by the addition of diethyl ether (ca. 100 mL) precipitated an orange solid, which was washed with diethyl ether (3 × 20 mL) and vacuum dried. **2.** Yield: 89% (591 mg). Anal. Calcd for RuC₅₄H₄₅F₆P₃O: C, 63.71; H, 4.45. Found: C, 63.92; H, 4.40. Conductivity (acetone, 20 °C): 119 Ω⁻¹ cm² mol⁻¹. IR (KBr, cm⁻¹): ν 837 (PF₆⁻). ³¹P{¹H} NMR (CD₂Cl₂): δ 39.74 (s) ppm. ¹H NMR (CD₂Cl₂): δ 3.76 (s, 3H, OCH₃), 5.25 (t, 1H, ³J_{HP} = 1.7 Hz, Ru=C=CH), 5.60 (d, 2H, ³J_{HH} = 2.8 Hz, H-1,3), 5.74 (t, 1H, ³J_{HH} = 2.8 Hz, H-2), 6.13 (m, 2H, H-4,7 or H-5,6), 6.77–7.46 (m, 36H, Ph, C₆H₄ and H-4,7 or H-5,6) ppm. ¹³C{¹H} NMR (CD₂Cl₂): δ 55.71 (s, OCH₃), 83.98 (s, C-1,3), 98.98 (s, C-2), 114.82 (s, CH of C₆H₄), 115.91 (s, C-3a,7a), 118.32 (s, C_β), 118.82 (s, C of C₆H₄), 123.62 and 128.68 (s, C-4,7 and C-5,6), 128.90–133.89 (m, Ph and CH of C₆H₄), 159.36 (s, C of C₆H₄), 353.39 (t, ²J_{CP} = 16.9 Hz, Ru=C_α) ppm. **3.** Yield: 92% (599 mg). Anal. Calcd for RuC₅₄H₄₅F₆P₃: C, 64.73; H, 4.52. Found: C, 65.02; H, 4.49. Conductivity (acetone, 20 °C): 115 Ω⁻¹ cm² mol⁻¹. IR (KBr, cm⁻¹): ν 838 (PF₆⁻). ³¹P{¹H} NMR (CD₂Cl₂): δ 39.59 (s) ppm. ¹H NMR (CD₂Cl₂): δ 2.33 (s, 3H, CH₃), 5.26 (s, 1H, Ru=C=CH), 5.62 (d, 2H, ³J_{HH} = 2.5 Hz, H-1,3), 5.77 (t, 1H, ³J_{HH} = 2.5 Hz, H-2), 6.13 (m, 2H, H-4,7 or H-5,6), 6.80–7.47 (m, 36H, Ph, C₆H₄ and H-4,7 or H-5,6) ppm. ¹³C{¹H} NMR (CD₂Cl₂): δ 21.24 (s, CH₃), 83.95 (s, C-1,3), 99.02 (s, C-2), 115.99 (s, C-3a,7a), 118.64 (s, C_β), 123.73 and 127.35 (s, C-4,7 and C-5,6), 128.89–137.56 (m, Ph and C₆H₄), 352.58 (t, ²J_{CP} = 16.4 Hz, Ru=C_α) ppm. **4.** Yield: 75% (517 mg). Anal. Calcd for RuC₅₉H₄₇F₆P₃: C, 66.60; H, 4.45. Found: C, 66.41; H, 4.52. Conductivity (acetone, 20 °C): 111 Ω⁻¹ cm² mol⁻¹. IR (KBr, cm⁻¹): ν 835 (PF₆⁻). ³¹P{¹H} NMR (CDCl₃): δ 38.86 (s) ppm. ¹H NMR (CDCl₃): δ 5.24 (s, 1H, Ru=C=CH), 5.65 (d, 2H, ³J_{HH} = 2.5 Hz, H-1,3), 5.86 (t, 1H, ³J_{HH} = 2.5 Hz, H-2), 6.13 (m, 2H, H-4,7 or H-5,6), 6.87–7.54 (m, 41H, Ph, C₆H₄ and H-4,7 or H-5,6) ppm. ¹³C{¹H} NMR (CDCl₃): δ 83.52 (s, C-1,3), 98.41 (s, C-2), 115.56 (s, C-3a,7a), 117.81 (s, C_β), 123.11 and 126.57 (s, C-4,7

(35) The decrease of the electron density at C_β and the increase at C_α associated with the transformation of the vinylidene moiety X-(η¹-C=CH₂) toward a X-(η¹-HC=CH) structure was estimated during the analysis of charge evolution in the fragments X = MnH₃⁴⁻ and Me⁺.^{5a}

(36) Oro, L. A.; Ciriano, M. A.; Campo, M.; Foces-Foces, C.; Cano, F. H. *J. Organomet. Chem.* **1985**, 289, 117–131.

(37) Lavastre, O.; Cabioch, S.; Dixneuf, P. H.; Vohlidal, J. *Tetrahedron* **1997**, 53, 7595–7604.

(38) Takahashi, S.; Kuroyama, Y.; Sonogashira, K.; Hagihara, N. *Synthesis* **1980**, 627–630.

and C-5,6), 127.15–140.01 (m, Ph and C₆H₄), 351.84 (t, ²J_{CP} = 16.4 Hz, Ru=C_α) ppm. **5**. Yield: 77% (504 mg). Anal. Calcd for RuC₅₃H₄₂F₇P₃: C, 63.28; H, 4.20. Found: C, 63.40; H, 4.16. Conductivity (acetone, 20 °C): 118 Ω⁻¹ cm² mol⁻¹. IR (KBr, cm⁻¹): ν 838 (PF₆⁻). ³¹P{¹H} NMR (CDCl₃): δ 39.33 (s) ppm. ¹H NMR (CDCl₃): δ 5.20 (s, 1H, Ru=C=CH), 5.62 (d, 2H, ³J_{HH} = 2.8 Hz, H-1,3), 5.88 (t, 1H, ³J_{HH} = 2.8 Hz, H-2), 6.08 (m, 2H, H-4,7 or H-5,6), 6.80–7.46 (m, 36H, Ph, C₆H₄ and H-4,7 or H-5,6) ppm. ¹³C{¹H} NMR (CDCl₃): δ 84.13 (s, C-1,3), 98.86 (s, C-2), 116.01 (s, C-3a,7a), 116.12 (d, ²J_{CF} = 20.7 Hz, CH of C₆H₄), 117.71 (s, C_β), 123.65 and 130.82 (s, C-4,7 and C-5,6), 128.77–133.93 (m, Ph and C₆H₄), 350.98 (t, ²J_{CP} = 16.9 Hz, Ru=C_α) ppm. **6**. Yield: 74% (493 mg). Anal. Calcd for RuC₅₃H₄₂F₆P₃Cl: C, 62.26; H, 4.14. Found: C, 62.40; H, 4.09. Conductivity (acetone, 20 °C): 109 Ω⁻¹ cm² mol⁻¹. IR (KBr, cm⁻¹): ν 839 (PF₆⁻). ³¹P{¹H} NMR (CD₂Cl₂): δ 38.68 (s) ppm. ¹H NMR (CD₂Cl₂): δ 5.20 (t, 1H, ⁴J_{HP} = 1.9 Hz, Ru=C=CH), 5.66 (d, 2H, ³J_{HH} = 2.7 Hz, H-1,3), 5.81 (t, 1H, ³J_{HH} = 2.7 Hz, H-2), 6.13 (m, 2H, H-4,7 or H-5,6), 6.77–7.52 (m, 36H, Ph, C₆H₄ and H-4,7 or H-5,6) ppm. ¹³C{¹H} NMR (CD₂Cl₂): δ 84.40 (s, C-1,3), 98.86 (s, C-2), 115.96 (s, C-3a,7a), 117.73 (s, C_β), 123.67 and 130.92 (s, C-4,7 and C-5,6), 126.29–134.30 (m, Ph and C₆H₄), 351.20 (t, ²J_{CP} = 17.1 Hz, Ru=C_α) ppm. **7**. Yield: 79% (572 mg). Anal. Calcd for RuC₅₃H₄₂F₆P₃I: C, 57.15; H, 3.80. Found: C, 57.21; H, 3.92. Conductivity (acetone, 20 °C): 118 Ω⁻¹ cm² mol⁻¹. IR (KBr, cm⁻¹): ν 839 (PF₆⁻). ³¹P{¹H} NMR (CD₂Cl₂): δ 38.48 (s) ppm. ¹H NMR (CD₂Cl₂): δ 5.18 (s, 1H, Ru=C=CH), 5.66 (d, 2H, ³J_{HH} = 2.7 Hz, H-1,3), 5.80 (t, 1H, ³J_{HH} = 2.7 Hz, H-2), 6.12 (m, 2H, H-4,7 or H-5,6), 6.60–7.53 (m, 36H, Ph, C₆H₄ and H-4,7 or H-5,6) ppm. ¹³C{¹H} NMR (CD₂Cl₂): δ 84.31 (s, C-1,3), 91.44 (s, C-1), 98.78 (s, C-2), 116.01 (s, C-3a,7a), 117.88 (s, C_β), 123.64 and 130.92 (s, C-4,7 and C-5,6), 127.58–138.14 (m, Ph and C₆H₄), 351.01 (t, ²J_{CP} = 17.1 Hz, Ru=C_α) ppm. **8**. Yield: 72% (480 mg). Anal. Calcd for RuC₅₃H₄₅F₆P₃O: C, 64.14; H, 4.40. Found: C, 64.21; H, 4.32. Conductivity (acetone, 20 °C): 114 Ω⁻¹ cm² mol⁻¹. IR (KBr, cm⁻¹): ν 833 (PF₆⁻), 1671 (C=O). ³¹P{¹H} NMR (CD₂Cl₂): δ 38.05 (s) ppm. ¹H NMR (CD₂Cl₂): δ 2.53 (s, 3H, CH₃), 5.26 (t, 1H, ⁴J_{HP} = 1.6 Hz, Ru=C=CH), 5.71 (d, 2H, ³J_{HH} = 2.7 Hz, H-1,3), 5.84 (t, 1H, ³J_{HH} = 2.7 Hz, H-2), 6.11 (m, 2H, H-4,7 or H-5,6), 6.83–7.78 (m, 36H, Ph, C₆H₄ and H-4,7 or H-5,6) ppm. ¹³C{¹H} NMR (CD₂Cl₂): δ 26.67 (s, CH₃), 84.45 (s, C-1,3), 98.76 (s, C-2), 116.15 (s, C-3a,7a), 118.19 (s, C_β), 123.67 and 126.61 (s, C-4,7 and C-5,6), 128.57–135.78 (m, Ph and C₆H₄), 197.07 (s, C=O), 350.64 (t, ²J_{CP} = 17.0 Hz, Ru=C_α) ppm. **10**. Yield: 81% (509 mg). Anal. Calcd for RuC₅₁H₄₇F₆P₃: C, 63.29; H, 4.89. Found: C, 63.15; H, 4.96. Conductivity (acetone, 20 °C): 112 Ω⁻¹ cm² mol⁻¹. IR (KBr, cm⁻¹): ν 835 (PF₆⁻). ³¹P{¹H} NMR (CDCl₃): δ 41.22 (s) ppm. ¹H NMR (CDCl₃): δ 0.84 (t, 3H, ³J_{HH} = 6.8 Hz, CH₃), 1.18 (m, 4H, CH₂), 2.01 (m, 2H, CH₂), 4.28 (t, 1H, ³J_{HH} = 7.7 Hz, Ru=C=CH), 5.37 (d, 2H, ³J_{HH} = 2.6 Hz, H-1,3), 5.75 (t, 1H, ³J_{HH} = 2.6 Hz, H-2), 5.99 and 7.19 (m, 2H each, H-4,7 and H-5,6), 6.80–7.48 (m, 30H, Ph) ppm. ¹³C{¹H} NMR (CDCl₃): δ 14.16 (s, CH₃), 21.48, 22.54, and 33.82 (s, CH₂), 83.64 (s, C-1,3), 99.18 (s, C-2), 113.28 (s, C_β), 115.22 (s, C-3a,7a), 123.41 and 130.24 (s, C-4,7 and C-5,6), 128.82–134.35 (m, Ph), 346.48 (t, ²J_{CP} = 15.7 Hz, Ru=C_α) ppm.

Synthesis of [Ru{=C=C(D)-4-F-C₆H₄}(η⁵-C₉H₇)(PPh₃)₂][PF₆] (**5-d**). D₂O (5 mL) was added to a solution of the vinylidene complex [Ru{=C=C(H)-4-FC₆H₄}(η⁵-C₉H₇)(PPh₃)₂][PF₆] (**5**) (200 mg, 0.198 mmol) in CD₂Cl₂ (5 mL) and the resulting mixture stirred at room temperature. Regular sampling and analysis by ¹H NMR showed complete H/D exchange of the acidic vinylidene proton after 5 h. The solvents were then removed under reduced pressure, and the resulting oily residue was dried in vacuo for 20 h to afford **5-d** as an orange solid in almost quantitative yield. NMR data for **5-d** are as follows. ³¹P{¹H} NMR (CD₂Cl₂): δ 39.90 (s) ppm. ¹H

NMR (CD₂Cl₂): δ 5.71 (d, 2H, ³J_{HH} = 2.4 Hz, H-1,3), 5.93 (t, 1H, ³J_{HH} = 2.4 Hz, H-2), 6.25 (m, 2H, H-4,7 or H-5,6), 6.82–7.57 (m, 36H, Ph, C₆H₄ and H-4,7 or H-5,6) ppm. ¹³C{¹H} NMR (CD₂Cl₂): δ 85.19 (s, C-1,3), 99.12 (s, C-2), 117.16 (s, C-3a,7a), 117.60 (d, ²J_{CF} = 19.5 Hz, CH of C₆H₄), 118.20 (t, ¹J_{CD} = 20.1 Hz, C_β), 124.51 and 132.12 (s, C-4,7 and C-5,6), 129.90–135.87 (m, Ph and C₆H₄), 353.11 (t, ²J_{CP} = 16.7 Hz, Ru=C_α) ppm.

Synthesis of [Ru{=C=C(H)Ph}(η⁵-C₉H₇)(PPh₃)₂][PF₆] (1b**)**. This complex, isolated as an orange solid, was prepared as described for **1¹⁵** starting from [RuCl(η⁵-C₉H₇)(PPh₃)₂] (100 mg, 0.13 mmol), NaPF₆ (44 mg, 0.26 mmol), and PhC≡CH (17 μL, 0.16 mmol). Yield: 79% (101 mg). Anal. Calcd for RuC₅₂¹³CH₄₃F₆P₃: C, 64.47; H, 4.38. Found: C, 64.21; H, 4.45. Conductivity (acetone, 20 °C): 115 Ω⁻¹ cm² mol⁻¹. IR (KBr, cm⁻¹): ν 837 (PF₆⁻). ³¹P{¹H} NMR (CD₂Cl₂): δ 39.14 (d, ²J_{PC} = 16.3 Hz) ppm. ¹H NMR (CD₂Cl₂): δ 5.33 (dt, ²J_{HC} = 3.4 Hz, ⁴J_{HP} = 1.1 Hz, Ru=C=CH), 5.68 (d, 2H, ³J_{HH} = 2.6 Hz, H-1,3), 5.85 (t, 1H, ³J_{HH} = 2.6 Hz, H-2), 6.17 (m, 2H, H-4,7 or H-5,6), 6.89–7.51 (m, 37H, Ph and H-4,7 or H-5,6) ppm. ¹³C{¹H} NMR (CD₂Cl₂): δ 86.04 (br, C-1,3), 101.04 (s, C-2), 118.06 (s, C-3a,7a), 120.67 (d, ¹J_{CC} = 62.1 Hz, C_β), 125.66 and 129.92 (s, C-4,7 and C-5,6), 129.40–135.96 (m, Ph), 353.56 (t, ²J_{CP} = 16.3 Hz, Ru=C_α) ppm.

Kinetic Measurements. ¹H and ³¹P{¹H} NMR spectra were obtained using a Bruker AC 300 P instrument. A weighed amount of vinylidene complexes **1–11** (11–20 mg) was dissolved in acetonitrile-*d*₃ (0.500 mL) in a 5 mm NMR tube. The samples were shaken to obtain clear solutions just before introduction into the NMR probe, and the experiment was started immediately afterward, after allowing about 1 min for thermal equilibration and experiment setup. A macro sequence of the Aspect 3000 software was used for the collection of fids at regular interval times, with an appropriate delay time being chosen depending on the substrate and temperature. The *k*_{obs} values for consumption of the vinylidene complexes or for product formation were obtained from a nonlinear least-squares regression analysis, by fitting the exponential dependence of concentration, *c*, calculated from the peak intensities of the ³¹P{¹H} NMR resonance of the starting complex, against time, according to the first-order rate equation (eqs 4 and 5). Within experimental error (10%), the same *k*_{obs} values were obtained from integration of the ³¹P NMR peaks with respect to P(*o*-tolyl)₃ as an internal standard, as checked for selected runs.

$$c_t = c_\infty + (c_0 - c_\infty) \exp(-k_{\text{obs}}t) \quad (4)$$

$$c_t = c_\infty - (c_\infty - c_0) \exp(-k_{\text{obs}}t) \quad (5)$$

The procedure yields values of *c*_∞, *k*_{obs}, and correlation coefficient *R*, which were ≥ 0.98. The values of *K* and Δ*G*^o for the equilibrium in eq 3 were calculated from the molar concentration values 0.022, 17.7, and 0.73 M of the ruthenium complexes **1** + **1a** overall, CD₃CN, and PhC≡CH, respectively.

Acknowledgment. This work was supported by the Ministerio de Educación y Ciencia (MEC) of Spain (Project CTQ2006-08485/BQU), by Consolider Ingenio 2010 (CSD2007-00006), and by CNR, Dipartimento di Progettazione Molecolare. V.C. thanks MEC and the European Social Fund for a “Ramón y Cajal” contract. M.B. thanks Arianna Antonucci for assistance in the kinetic measurements.

Supporting Information Available: ³¹P{¹H} and ¹³C{¹H} NMR spectra of the enriched vinylidene complex **1b** and of the reaction solution after demetalation, Eyring plot of **1**, and first-order fits of selected kinetic measurements. This material is available free of charge via the Internet at <http://pubs.acs.org>.

OM800484U